

## RESEARCH ARTICLE

# Global cropland nitrous oxide emissions in fallow period are comparable to growing-season emissions

Ziyin Shang<sup>1</sup>  | Xiaoqing Cui<sup>2</sup>  | Kees Jan van Groenigen<sup>3</sup>  | Matthias Kuhnert<sup>4</sup>  | Mohamed Abdalla<sup>4</sup>  | Jiafa Luo<sup>5</sup>  | Weijian Zhang<sup>1</sup>  | Zhenwei Song<sup>1</sup>  | Yu Jiang<sup>6</sup>  | Pete Smith<sup>4</sup>  | Feng Zhou<sup>7,8</sup> 

<sup>1</sup>Institute of Crop Sciences, Chinese Academy of Agricultural Sciences, Beijing, China

<sup>2</sup>School of Grassland Science, Beijing Forestry University, Beijing, China

<sup>3</sup>Department of Geography, College of Life and Environmental Sciences, University of Exeter, Exeter, UK

<sup>4</sup>Institute of Biological and Environmental Sciences, University of Aberdeen, Aberdeen, UK

<sup>5</sup>AgResearch Ruakura, Hamilton, New Zealand

<sup>6</sup>College of Agronomy, Nanjing Agricultural University, Nanjing, China

<sup>7</sup>Laboratory for Earth Surface Processes, College of Urban and Environmental Sciences, Peking University, Beijing, P.R. China

<sup>8</sup>College of Geography and Remote Sensing, Hohai University, Nanjing, China

## Correspondence

Feng Zhou, Laboratory for Earth Surface Processes, College of Urban and Environmental Sciences, Peking University, Beijing, P.R. China and College of Geography and Remote Sensing, Hohai University, Nanjing, China.  
Email: [zhouf@pku.edu.cn](mailto:zhouf@pku.edu.cn)

## Funding information

National Natural Science Foundation of China, Grant/Award Number: 42225102, 42361144876, 42301059, 32172129 and 42207378; The Youth innovation Program of Chinese Academy of Agricultural Sciences, Grant/Award Number: Y2023QC02; National Key Research and Development Program of China, Grant/Award Number: 2021YFD1700801 and 2022YFD2300400; Technology Research System-Green Manure, Grant/Award Number: CARS-22-G-16

## Abstract

Croplands account for ~ one-third of global anthropogenic nitrous oxide (N<sub>2</sub>O) emissions. A number of recent field experiments found substantial fallow-period N<sub>2</sub>O emissions, which have been neglected for decades. However, the global contribution of the fallow-period emissions and the associated drivers remain unclear. Based on 360 observations across global agroecosystems, we simulated the ratio of the fallow to the whole-year N<sub>2</sub>O emissions ( $R_{\text{fallow}}$ ) by developing a mixed-effect model and compiling cropping-system-specific input data. Our results revealed that the mean global gridded  $R_{\text{fallow}}$  was 44% (15%–75%, 95% confidence interval), with hotspots mainly in the northern high latitudes. For most cropping systems, soil pH was the dominant driver of global variation in  $R_{\text{fallow}}$ . Global cropland emission factors (i.e., the percentage of fertilizer N emitted as N<sub>2</sub>O, EFs) in EF-based models doubled to 1.9% when the fallow-period N<sub>2</sub>O emissions were included in our simulation, similar to EFs estimated by process-based and atmospheric inversion models (1.8%–2.3%). Overall, our study highlights the importance of fallow-period N<sub>2</sub>O emissions in annual totals, especially for single cropping systems and croplands in acidic areas. To accurately estimate N<sub>2</sub>O emissions for national greenhouse gas inventories, it is crucial to update current EFs with full consideration of the fallow-period N<sub>2</sub>O emissions in the Intergovernmental Panel on Climate Change (IPCC) Tier 1 method.

## KEYWORDS

cropping system, greenhouse gas, inventory, nitrous oxide, non-growing season, simulation, spatial variation

Ziyin Shang and Xiaoqing Cui should be considered joint first author.

## 1 | INTRODUCTION

$\text{N}_2\text{O}$  is one of the major agricultural greenhouse gases (GHGs) and the most significant atmospheric ozone-depleting substance (Ravishankara et al., 2009). Most countries in the world are requested by the United Nations Framework Convention on Climate Change (UNFCCC) to compile and report their national GHG and  $\text{N}_2\text{O}$  inventories (Deng et al., 2022). About one-third of anthropogenic  $\text{N}_2\text{O}$  emissions are derived from croplands (Tian et al., 2020). Cropland  $\text{N}_2\text{O}$  emissions are mainly from microbial processes in soils (Butterbach-Bahl et al., 2013), such as nitrification and denitrification, contributing to N loss from the management-driven climate-soil-crop systems. Management practices, such as N fertilizer inputs, cropping period and cropping system selection, play important roles in the cropland  $\text{N}_2\text{O}$  emissions (Cui et al., 2021). Therefore, accurate estimates of regional cropland  $\text{N}_2\text{O}$  emissions are crucial for developing and adjusting agricultural management strategies aimed at mitigating both climate change and ozone depletion.

Cropland  $\text{N}_2\text{O}$  emission can be estimated through different methodologies (e.g., EF-based, atmospheric inversion and process-based models) with large discrepancies. One potential factor for the underestimation of  $\text{N}_2\text{O}$  emissions in GHG inventories is the omission of emissions during fallow (non-growing) periods (Shang et al., 2020). Most  $\text{N}_2\text{O}$  emission fluxes used for building the EF-based inventories are measured during growing seasons rather than whole years (Cui et al., 2021; Shang et al., 2020), since the fallow periods usually come with cold weather and limited residual N. However, field observations suggest that fallow-period  $\text{N}_2\text{O}$  emissions accounted for 36% on average of the annual emissions for wheat and maize in Canada (Ekwunife et al., 2022; Pelster et al., 2022), and even more for rice paddies in Asia. Since the soil condition in fallow rice paddies after harvest drainage is usually moist but non-waterlogged, it can stimulate  $\text{N}_2\text{O}$  production and inhibit the reduction of  $\text{N}_2\text{O}$  to  $\text{N}_2$  in denitrification (Shang et al., 2020). To convert growing-season emissions to annual emissions, a limited number of correction factors are currently available for a few cropping systems, or are restricted for application in specific regions (Pelster et al., 2022). Therefore, it is critical to quantify the contribution of fallow-period  $\text{N}_2\text{O}$  emissions to the annual total emissions at a global scale and to provide reliable correction factors.

The contribution of the fallow period to annual total  $\text{N}_2\text{O}$  emissions varies with management practices, soil properties and climatic conditions. The type of cropping system is an integrated indicator of the specific crops cultivated within a year, management practices and the surrounding environmental conditions. For example, the single rice cropping system, which is generally adopted in humid high-altitude regions, has a longer and cooler fallow period compared with double rice cropping in humid low-altitude regions. In contrast, rice-wheat and maize-wheat systems have the shortest fallow periods in all cropping setups, ranging from 2 to 3 months. A recent study revealed that precipitation and temperature are key driving factors for fallow-period  $\text{N}_2\text{O}$  emissions in the US Midwest (Yang

et al., 2023). In a previous study, we revealed the role of factors like crop types, annual precipitation, soil pH and soil organic carbon in determining the difference in  $\text{N}_2\text{O}$  EF caused by the omissions of fallow period (Shang et al., 2020). However, the global pattern of the contribution of fallow-period  $\text{N}_2\text{O}$  emissions and the associated drivers remain unclear. This is mainly due to the lack of a quantitative model and a fallow calendar for different cropping systems. It hinders our understanding of the importance of fallow-period  $\text{N}_2\text{O}$  emissions and our ability to accurately estimate national and global  $\text{N}_2\text{O}$  emissions in GHG inventories.

To address these gaps, we quantified the ratio of fallow to whole-year emissions ( $R_{\text{fallow}}$ ) using a mixed-effect model that connected crop-specific  $R_{\text{fallow}}$  variations to climate, soil and agricultural management practices. We conducted our analysis using 360 chamber-based field observations, spanning 53 sites globally. By combining the spatial datasets of the physical areas of multiple cropping systems, crop calendar and crop-specific fertilizer N inputs (including synthetic fertilizers, manure and crop residues), we compiled datasets of gridded N input and the duration of fallow period for each cropping system. Using the datasets with management and environmental variables, and the model constrained by the global observations, we mapped crop-specific  $R_{\text{fallow}}$  at the spatial resolution of five-arcminute and identified the key drivers of spatial variations in  $R_{\text{fallow}}$ . Finally, we converted growing-season  $\text{N}_2\text{O}$  emissions to whole-year emissions at global scale, aiming to reconcile the discrepancies in cropland  $\text{N}_2\text{O}$  emissions estimated by different methodologies.

## 2 | DATA AND METHODS

### 2.1 | Observations for quantifying $R_{\text{fallow}}$

We compiled a global observation dataset consisting of 360  $R_{\text{fallow}}$  values from currently available literature databases and online data repositories (Text S1). The observed  $R_{\text{fallow}}$  values were calculated based on fallow and annual  $\text{N}_2\text{O}$  emissions for different single (i.e., legumes, maize, wheat, rice and others) or double cropping systems (i.e., rice-rice, rice-upland and upland-upland). Triple cropping systems (e.g., rice-rice-rapeseed) are very rare in modern global food production (Waha et al., 2020), and their fallow-period  $\text{N}_2\text{O}$  emission measurements are rather limited. Thus, these systems were excluded from the analysis. Studies with the following measurements were further excluded: (i) experiments conducted in laboratories, pots or greenhouses, (ii) measurements conducted in organic (peaty) soils where  $\text{N}_2\text{O}$  are much higher than those in mineral soils (IPCC, 2006) and (iii) measurements with the use of controlled-release fertilizers, nitrification inhibitors or urease inhibitors. The full dataset is a combination of data from 57 sites globally and 49 peer-reviewed papers and dissertations, including 71 observations for rice-rice, 25 for rice-upland, 20 for upland-upland systems, 25 for legumes, 49 for maize, 75 for wheat, 60 for rice and 35 for other single cropping systems (Figure S1; Table S1).

For each record, four categories of information were collected: (i) N<sub>2</sub>O emissions, (ii) climatic conditions, (iii) soil properties, (iv) management practices and (v) sampling information. The N<sub>2</sub>O emissions for the whole year and fallow period were obtained from the studies identified to calculate the ratios. The fallow period was defined as the period between harvesting crop and sowing or transplanting the next crop. Climatic conditions include mean annual air temperature (MAT) and mean annual precipitation (MAP), fallow-period mean air temperature (FT) and precipitation (FP). Soil properties contain soil organic carbon content (SOC), pH, bulk density (BD) and clay and sand content. Along with climatic conditions, these soil properties influence the substrate availability and soil aeration and determine the rates of microbial processes underlying N<sub>2</sub>O emissions (Bouwman et al., 2013; Butterbach-Bahl et al., 2013). Management practices include cropping system type, N fertilizer application rate and fallow duration. These practices are significant due to their known impacts on agroecosystem C and N cycling and fallow-period emissions (Cui et al., 2021; Shang et al., 2020). Sampling information includes mean sampling interval during fallow period, and whether sampling frequency is intensified at N<sub>2</sub>O flux peaks when the mean interval during fallow period is greater than 7 days (Text S2; Figure S2). Most information was obtained from the original papers; values not reported in the original papers were obtained from climate and soil databases (Text S1). The definition and unit of each variable and related information can be found in Table S2.

The representativeness of the observations in terms of a per-pixel representation of the relative proportion of interpolation, was assessed according to the method van den Hoogen et al. (2019). To investigate how well our compiled observation dataset spread throughout the full multivariate covariate space (for all soil, climate and management practice-related variables in the model), we performed a principal component analysis (PCA)-based approach. Firstly, we utilized the centring values, scaling values, and eigenvectors to transform the composite image into the same PCA space. Subsequently, we generated convex hulls for each of the bivariate combinations from the first seven principal components, which collectively accounted for over 90% of the sample space variation. Based on the coordinates of these convex hulls, we classified each pixel as falling within or outside of them, that is a per-pixel representation of the relative proportion of interpolation and extrapolation. The relative percentage of interpolation reflects how adequately our dataset captured the multivariate covariate space of the global layers.

## 2.2 | Linear mixed-effect model for R<sub>fallow</sub>

We developed a linear mixed-effect (LME) model to generate an interpretable regression of R<sub>fallow</sub> in response to various environmental and management-related factors. The LME is capable of capturing the fixed effects quantified by the key factors and identifying the random effects for N<sub>2</sub>O emissions, which can be represented by the sites (Cui et al., 2021). First, to enhance the ability of model to

capture the variance, R<sub>fallow</sub> was converted from the original range of 0 to 1 (11 negative values were excluded) to an infinite range with normal distribution using Equation (E1), and independent variables were re-scaled using “scale” function in R v.4.2.2.

Second, partial correlation and a generalized boosted regression mode (GBM) were used to determine the key variables for the model. GBM was performed using the “gbm” package in R v.4.2.2. GBM is an ensemble tree-based method that combines multiple weak models to form a single strong model, based on the prior trees, to quantify the relative importance of each variable. Third, the Akaike information criterion (AIC) was implemented by adding variables based on the priority order and the most relevant variables for the LME model were selected to avoid over-fitting (Table S3). Fourth, we checked for interactions among variables. An analysis of variance (ANOVA) test indicated that the model with an interaction between cropping system type and N fertilization rate outperformed other models. Eventually, the LME model included cropping system type, soil pH, N fertilization rate and fallow duration as fixed-effect terms. Additionally, the model incorporated the site identity in the intercept as a random-effect term (Equation E2). The interaction between the cropping system and N application rate was considered in the LME model through distinguishing slopes corresponding to different cropping systems and N fertilization rates. R<sub>fallow</sub> for each cropping system was then quantified as follows:

$$R_{\text{fallow } i} = e^{y_i} / (1 + e^{y_i}), \quad (\text{E1})$$

$$y_i = (\alpha + \varphi_i) + (\beta + \theta_i) \times \text{Nrate}_i + \gamma \times \text{pH} + \delta \times D_i + (1 | \text{Site}) + \varepsilon_i, \quad (\text{E2})$$

where  $y$  is the mediator between R<sub>fallow</sub> and driving variables selected to facilitate the normal distribution of R<sub>fallow</sub>;  $i$  denotes the type of eight cropping systems mentioned above; Nrate is nitrogen (N) fertilizer application rate (kg N ha<sup>-1</sup>); pH is soil pH;  $D$  is the duration of a fallow period in days; Site means the location of the observational field experiments;  $\alpha$ ,  $\beta$ ,  $\gamma$ ,  $\delta$ ,  $\varphi$  and  $\theta$  are variable coefficients;  $\varepsilon$  is the residual term.  $(\alpha + \varphi_i) + (\beta + \theta_i) \times \text{Nrate}$  represents the interactive effect between N fertilizer application rate and cropping system, allowing for the eight different cropping systems in our analysis to vary in their response (i.e., slope and intercept) to changes in N application rate;  $1 | \text{Site}$  represents the random-effect term in the mixed-effect model. All the model parameters were quantified using the “lmer” function in the R package “lme4”.

The model was trained and tested on a tenfold cross-validation repeated 10 times. Cross-validation has been widely used in many studies (Bo et al., 2022; Malakouti, 2023; Viscarra Rossel et al., 2019). The tenfold cross-validation involves splitting all the observations into 10 equal parts, training the model on nine parts and testing it on the remaining part. This process is repeated 10 times, with each part used as the test set exactly once. To avoid bias due to subsets randomly divided, we repeated the above steps by 10 times for possible subdivisions. The advantage of cross-validation is that it provides a more reliable estimate of model performance compared with a single train-test split. By averaging the results of different test

sets, it reduces the variability of a single partition and provides a more accurate assessment of how the model is likely to perform on unseen data. The coefficients of the model based on 100 trainings were stored for spatial prediction. The performance and robustness of the model were evaluated by comparing simulated and observed  $R_{\text{fallow}}$  by cropping system, using the 1:1 line,  $R^2$  of fixed effect ( $R^2_c$ ),  $R^2$  of mixed effect ( $R^2_m$ ), slope and root mean square error (RMSE). Additionally, the responses of  $R_{\text{fallow}}$  to the key variables selected were estimated for each cropping system in the sensitivity tests, with the uncertainty of one standard error using the “sjPlot” package in R. The ranges of the key variables in the sensitivity tests were constrained by those of the observations.

### 2.3 | Global prediction of $R_{\text{fallow}}$

The global patterns of  $R_{\text{fallow}}$  for each cropping system were simulated using the “predict” function in the LME model at a spatial resolution of 5-arcmin, which were driven by the duration of the fallow period, the N application rate and the soil pH. Soil pH was derived directly from the HWSD v1.2 at a resolution of 30-arc-s. Data regarding the spatial distribution of the eight cropping systems, the duration of the fallow period and the N application rate for each cropping system were specifically compiled for this study.

Physical areas of cropping systems were derived from Waha et al. (2020), which reported multiple attributes including cropping intensity (single, double or triple), types of crops grown in the system (out of a pool of 26 crops from MIRCA2000 (Monfreda et al., 2008)). Crops without planting and harvesting calendars (e.g., citrus and grapes) were excluded from this study. In the end, 45 out of the initial 70 cropping systems were identified and obtained for this study. The global gridded physical areas for these 45 cropping systems were first resampled from 30' × 30' resolution to a 5' × 5' resolution using the nearest resampling method, then directly summed to obtain the physical area for each of the eight cropping systems. We grouped the double cropping systems into rice-rice, rice-upland and upland-upland systems, the single cropping systems into legumes, maize, wheat, rice and the remaining falling under the other cropping system, producing a total of eight cropping systems. We did not distinguish between rain-fed and irrigated systems.

Crop planting and harvesting dates from Sacks et al. (2010) were used as the reference to establish the duration of the fallow period for each cropping system. We first classified each of the obtained 45 cropping system layers as either a single or double cropping. For single cropping systems, the duration of the fallow period in each grid cell was calculated as the interval between the harvesting (H) and planting (P) dates of the corresponding crop, as provided by Sacks et al. (2010) (Equation E3).

$$FDs_{ij} = \begin{cases} 365 - H_{ij} + P_i, & P_{ij} < H_{ij} \\ P_{ij} - H_{ij}, & P_{ij} > H_{ij}, \end{cases} \quad (\text{E3})$$

where  $FDs_{ij}$  represents the duration of the fallow period for cropping system  $i$  in grid cell  $j$ ;  $H_{ij}$  and  $P_{ij}$  correspond to the harvesting date and planting date, respectively, for crop  $i$  in grid cell  $j$ .

For double cropping systems, the duration of the fallow period was calculated as the period without a crop actively growing within a calendar year. For each grid cell, the planting and harvesting dates for both the initial and subsequent crops in the rotation were identified. The duration of the fallow period for each double cropping system was then calculated accordingly by Equation (E4), as shown below.

$$FDs_{ij} = \begin{cases} P_{i_2j} - H_{i_1j} + 365 - H_{i_2j} + P_{i_1j}, & P_{i_1j} < H_{i_1j}, P_{i_2j} < H_{i_2j} \\ P_{i_2j} - H_{i_1j} + P_{i_1j} - H_{i_2j}, & P_{i_1j} < H_{i_1j}, P_{i_2j} > H_{i_2j} \\ P_{i_2j} - H_{i_1j} + P_{i_1j} - H_{i_2j}, & P_{i_1j} > H_{i_1j}, P_{i_2j} < H_{i_2j}, \end{cases} \quad (\text{E4})$$

where  $FDs_{ij}$  represents the duration of the fallow period for double cropping system  $i$  in grid cell  $j$ ;  $H_{i_1j}$ ,  $P_{i_1j}$ ,  $H_{i_2j}$  and  $P_{i_2j}$  correspond to the harvesting date and planting date for the first crop  $i_1$  in cropping system  $i$  in grid cell  $j$ , harvesting date and planting date for the second crop  $i_2$  in cropping system  $i$  in grid cell  $j$ , respectively. Lastly, the average duration of the fallow period for the eight cropping systems was obtained by weighting the physical areas of the different cropping systems.

Crop-specific N application rates per unit of harvested area and total N inputs from Adalibieke et al. (2023) were used to calculate the N application rates per unit of physical area for the eight cropping systems in our study. Firstly, we re-organized the above-mentioned physical areas of the 45 cropping systems into 15 crop groups (without accounting for differences in cropping frequency) out of 21 crops from Adalibieke et al. (2023). To address the differences in the physical area reported by Waha et al. (2020) and Adalibieke et al. (2023), missing N application rates for some specific physical areas in 2000 were imputed from nationally averaged N application rates, with the sum of N inputs for a crop and a country kept consistent as the original dataset (Adalibieke et al., 2023). N application rates per physical hectare were calculated for the 45 cropping systems. For a single cropping system, it was set to be the N application rate per harvested hectare of the corresponding crop, while for a double cropping system, the rate was equal to the sum of N application rates per harvested hectare for the corresponding first and second crops. Next, total N application inputs for the eight cropping systems investigated at each grid were aggregated by summing the products of the corresponding physical areas and N application rates from 45 cropping systems. Lastly, the N application rate per unit of physical area for each cropping system was generated by dividing the total N input by the corresponding physical area. The maximum N application rates were capped at 1000 and 2000 kg N ha<sup>-1</sup> for single and double cropping systems to avoid extremes, respectively.

We conducted 100 simulations of global  $R_{\text{fallow}}$  with the 100 sets of coefficients from the tenfold cross-validation repeated 10 times and then obtained the global prediction by averaging the predictions



from the 100 simulations (Viscarra Rossel et al., 2019). To calculate the weighted  $R_{\text{fallow}}$  for all cropping systems, we first calculated the mediator  $y$  for each cropping system and then averaged them based on their corresponding areas to get the weighted  $y$ . Finally, we transformed the weighted  $y$  to weighted  $R_{\text{fallow}}$  according to Equation (E1). In this case, we prefer to weight  $y$  rather than  $R_{\text{fallow}}$  because  $y$  is more sensitive to small differences among cropping systems with its infinite range. For the global prediction of  $R_{\text{fallow}}$ , their results are quite comparable (Figure S3) with almost the same mean values (mean  $\pm$  standard error of the mean:  $44.65 \pm 0.23\%$  and  $44.03 \pm 0.24\%$  for weighted  $R_{\text{fallow}}$ -based and weighted  $y$ -based methods respectively).

For the attribution of spatial variation in  $R_{\text{fallow}}$ , the dominant driver was defined as the factor with the largest absolute value of the partial correlation coefficient (par) in each grid cell, where par between  $R_{\text{fallow}}$  and predictors is done for  $3.75^\circ \times 3.75^\circ$  moving windows (Beer et al., 2010; Cui et al., 2021; Peng et al., 2013). To identify the dominant driver for all cropping systems, we multiplied the area percentage of each cropping system (i.e., the ratio of area for single rice to the area for all cropping systems) and the par of each factor for that system. Then, the factor with the largest absolute

value of par across all cropping systems was regarded as the most important variable determining the variation of  $R_{\text{fallow}}$ .

### 3 | RESULTS AND DISCUSSION

#### 3.1 | Modelling performance and response functions

Soil pH, cropping system type, N application rate and fallow duration were identified as the most important determinants of  $R_{\text{fallow}}$  than the environmental factors (i.e., soil sand and clay content, BD, SOC, MAP, MAT, FP and FT) included in our analysis (Figure 1a; Figure S4; Table S7). The repeated tenfold cross-validation results indicate that LME model, with the four most important factors as fixed effects and site as a random effect, captured 63% of the observed variation in  $R_{\text{fallow}}$  (Figure 1b). The combination of the four key fixed effects, that is, soil pH, cropping system, N application rate and fallow duration, explained 41% of the observed variation in  $R_{\text{fallow}}$ . This means that the fixed effect in the model developed explained more variation in  $R_{\text{fallow}}$  than the random

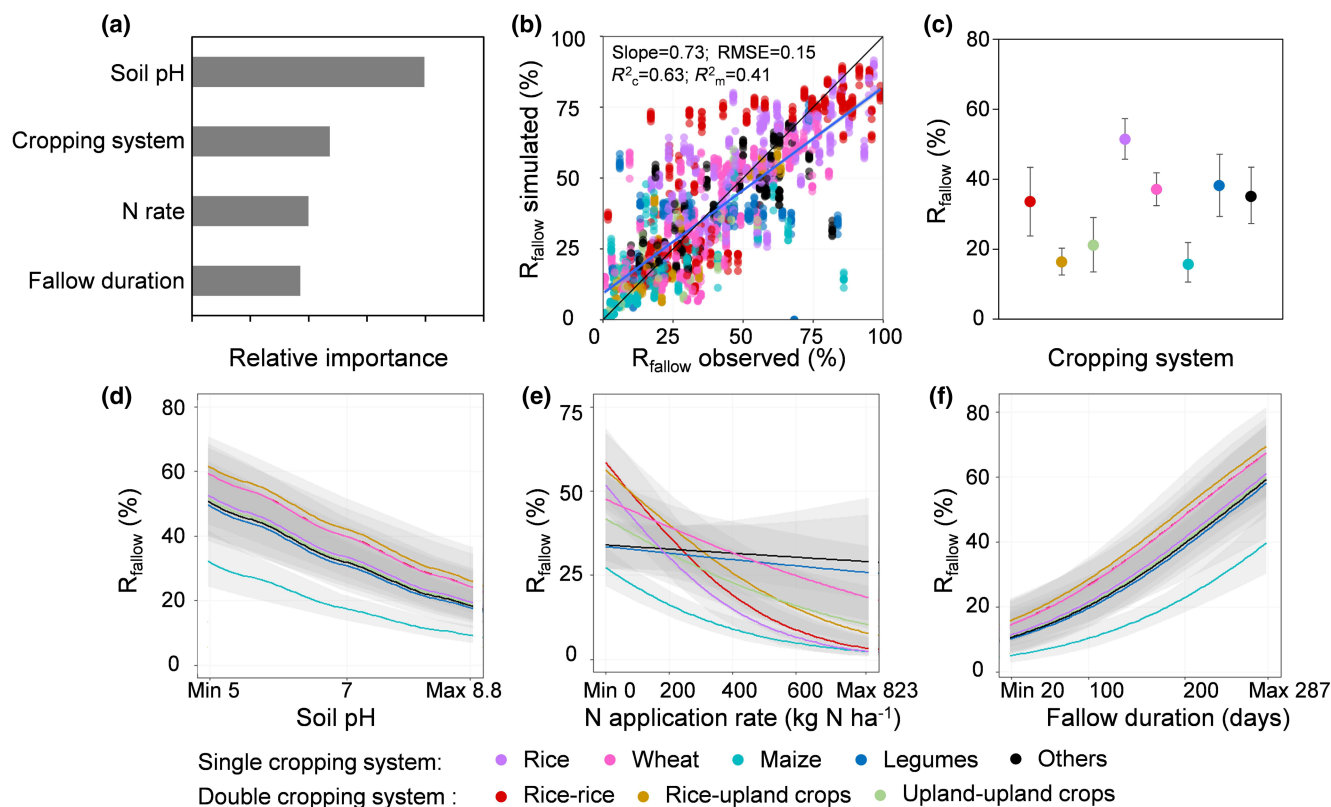


**FIGURE 1** Relative importance of selected variables (a), model performance (b) and the sensitivity of variable (e–f) for  $R_{\text{fallow}}$ . The four most important variables (i.e., soil pH, cropping system type, N application rate and fallow duration) were identified by partial correlation and generalized boosted regression mode, and selected in the mixed-effect model based on model AIC. The model was evaluated by  $R^2$  of fixed effect ( $R^2_c$ ),  $R^2$  of mixed effect ( $R^2_m$ ) and root mean square error (RMSE) based on a repeated tenfold cross-validation. The mean and error bar of 95% confidence interval were generated by bootstrapping resampling. The shade of sensitivity curve represents one standard error. The colour indicates cropping system type for a whole year.

effect did (Text S3). The slope between simulated and observed  $R_{\text{fallow}}$  is 0.73. These results are comparable with those using all the observations for both training and testing (Table S4). The representativeness analysis shows that the observations used for model development covered the vast majority of global variations, with 76% of global pixel values falling within the sampled range of at least 90% of all bands (Figure S5). Together, the results indicate that our model is effective and robust (Cui et al., 2021; Philibert et al., 2012). The corresponding means and standard errors of the model coefficients are listed in Table S5.

Among the eight cropping systems included in our analysis, the results show that the single rice system had the largest  $R_{\text{fallow}}$  at  $53 \pm 6\%$  (mean  $\pm$  95% confidence interval of the mean), followed by double rice-rice ( $46 \pm 7\%$ ), single other crops ( $39 \pm 7\%$ ), legumes ( $38 \pm 9\%$ ), wheat ( $37 \pm 5\%$ ), rice-upland ( $30 \pm 8\%$ ), upland-upland ( $21 \pm 8\%$ ) and single maize cropping systems ( $16 \pm 5\%$ ) (Figure 1c). Single cropping systems generally showed greater  $R_{\text{fallow}}$  than double cropping systems. Rice-dominated cropping systems (i.e., single rice and double rice-rice) exhibited larger  $R_{\text{fallow}}$  than the other systems.

Cropping system type is an integrated indicator representing local management practices and environmental conditions. Its influence can be largely attributed to factors such as MAT, MAP and fallow duration, which collectively captured 50%–99% of the variations observed for all cropping systems (Table S6). For instance, the single rice system in temperate and subtropical climate areas had the longest fallow duration (223 days for single rice compared with 159 days for the remainder systems). The associated moisture soil conditions after harvest drainage in this extended fallow period are favourable for  $\text{N}_2\text{O}$  emissions (Shang et al., 2020). In contrast, upland-upland and rice-upland cropping systems, which have the shortest fallow durations (62 and 114 days on average, respectively) and relatively lower soil moisture levels, which limits  $\text{N}_2\text{O}$  emissions during the fallow period.

Sensitivity tests indicated that  $R_{\text{fallow}}$  was negatively correlated with soil pH (Figure 1d) but positively correlated with the fallow duration (Figure 1f). Specifically,  $R_{\text{fallow}}$  in double rice-rice, rice-upland and wheat cropping systems responded more strongly to variations in soil pH and fallow duration than other cropping systems, while the single maize appeared at the lower end of all response curves (Figure 1d,f). The results indicate that  $R_{\text{fallow}}$  for rice-related cropping systems was more sensitive to N application rate than the other cropping systems, especially at N application rates  $<400 \text{ kg N ha}^{-1}$  (Figure 1e). This is probably because rice-related cropping systems had higher initial  $R_{\text{fallow}}$  (without N fertilization) than other cropping systems, due to the moist soil conditions during fallow period promoting  $\text{N}_2\text{O}$  emissions. Fertilizer N additions further increased growing-season  $\text{N}_2\text{O}$  emissions, which contributed the most to annual emissions, thereby reducing  $R_{\text{fallow}}$ . Together, these results suggest that the underestimation of cropland  $\text{N}_2\text{O}$  emission inventory based on EF methodologies, due to the omission of fallow-period  $\text{N}_2\text{O}$  emissions, can be potentially exaggerated for rice-related systems, especially at low levels of N fertilizer inputs.

### 3.2 | Spatial pattern of $R_{\text{fallow}}$

It is estimated that global average value of  $R_{\text{fallow}}$  (i.e., weighted by areas of global cropping systems and expressed as a percentage) was 44.0%, with a 95% confidence interval (CI) ranging from 14.5% to 74.6% (Table 1). The highest  $R_{\text{fallow}}$  was 56.6% (28.3%–81.1%) for single wheat cropping, followed by 52.3% (14.1%–79.7%) for rice, 48.8% (27.0%–71.6%) for legumes, 44.9% (23.6%–68.7%) for others, 34.6% (8.5%–65.4%) for maize, 26.2% (1.3%–61.5%) for double rice-rice, 12.4% (1.9%–30.2%) for rice-upland crops and 10.5% (1.6%–24.1%) for upland-upland crops (Table 1). The hotspots of high  $R_{\text{fallow}}$  ( $>60\%$ ) estimated were concentrated in northern high-altitude areas, the Amazon Plain and Southeast Asia (e.g., Myanmar, Thailand and Laos), while low  $R_{\text{fallow}}$  ( $<13\%$ ) areas were mainly located in southern high-altitude areas (e.g., Southern Africa, America and Australia), the North China Plain, Mexico and the Southwestern United States. The areas with high  $R_{\text{fallow}}$  were dominated by single wheat or rice-related cropping systems, those with low  $R_{\text{fallow}}$  were mostly covered by other upland crops (Sacks et al., 2010; Waha et al., 2020).

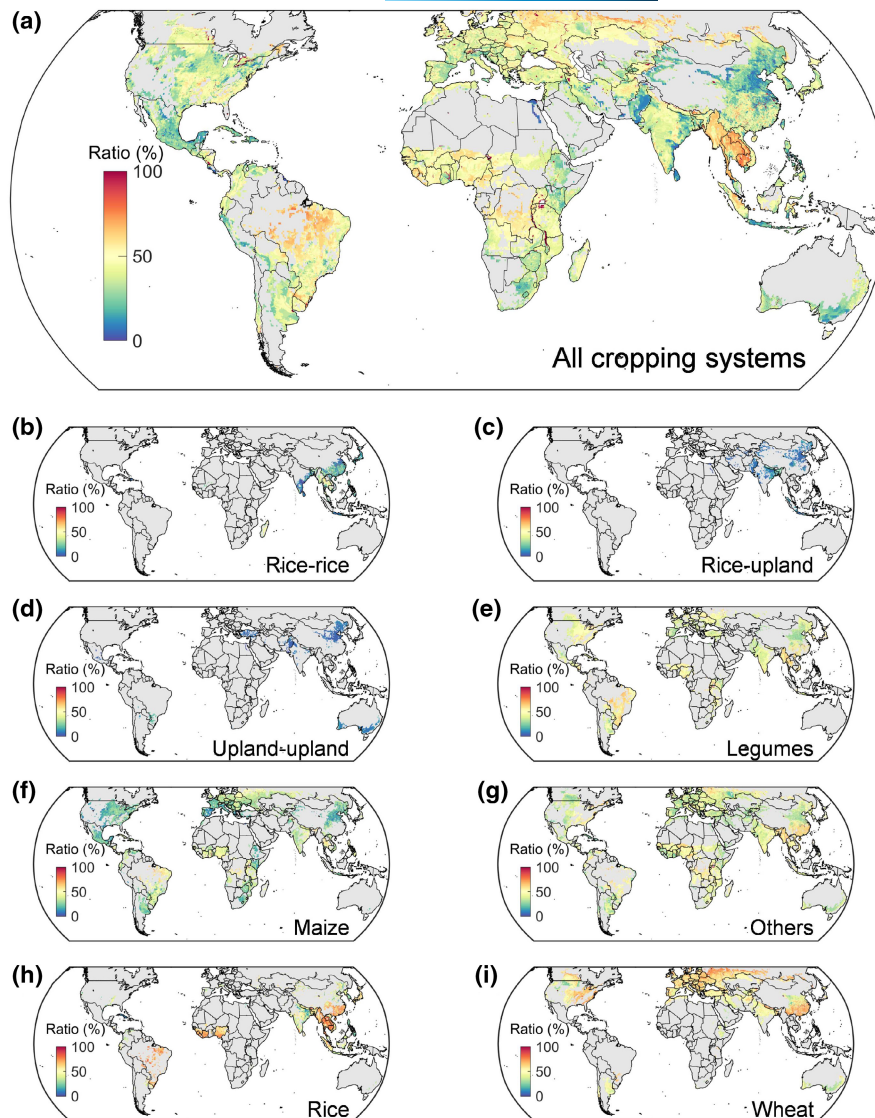
We found high  $R_{\text{fallow}}$  was concentrated in northern high-altitude areas. These areas generally have lower soil pH and more areas of single cropping systems (e.g., wheat, maize and other crops) (Figure S6). Based on partial correlation of observations, lower soil pH is significantly related to greater  $R_{\text{fallow}}$  ( $r = -.36$ ,  $p < .001$ , Table S7). Additionally, pH was strongly and negatively related to simulated  $R_{\text{fallow}}$  across all cropping systems at global scale (Figure S7) and was identified as the dominant driver of simulated  $R_{\text{fallow}}$  over other factors in major high-altitude areas (Figure 3). Single cropping system in northern high-altitude areas generally have longer fallow period and greater  $R_{\text{fallow}}$  than double cropping systems.

The results indicate that cropping systems showed distinctive spatial variations in  $R_{\text{fallow}}$  (Figure 2b–i). The  $R_{\text{fallow}}$  estimated for double rice-upland and upland-upland crops (mean  $\pm$  standard error of the mean:  $12.4 \pm 0.2$  and  $10.5 \pm 0.1\%$ , respectively) were only a quarter of the  $R_{\text{fallow}}$  observed for other cropping systems ( $46.4 \pm 0.3\%$ ), especially in regions such as the North China Plain, Northeastern China, the Indus Plain, Turkey and Mexico. In

TABLE 1 Mean and 95% confidence interval (CI) for the stimulated  $R_{\text{fallow}}$  by cropping system.

Category	Cropping system	Mean (%)	95% CI (%)
Single	Wheat	56.5	28.3–81.1
	Rice	52.3	14.1–79.7
	Legumes	48.8	27.0–71.6
	Others	44.9	23.6–68.7
	Maize	34.6	8.5–65.4
Double	Rice-rice	26.2	1.3–61.5
	Rice-upland crops	12.4	1.9–30.2
	Upland-upland crops	10.5	1.6–24.1
Global		44.0	14.5–74.6

**FIGURE 2** Global patterns of  $R_{\text{fallow}}$  (a) Ratios weighted by areas of different cropping systems, including the double (rice-rice (b), rice-upland crops (c) and upland-upland crops (d)) and single (legumes (e), maize (f), others (g), rice (h) and wheat (i)). Ratios were predicted with a linear mixed-effect model. Values are shown only where the proportion of harvested area within the grid cell is greater than 0.5%. Map lines delineate study areas and do not necessarily depict accepted national boundaries.



contrast,  $R_{\text{fallow}}$  for single rice and wheat systems ( $52.3 \pm 0.3$  and  $56.6 \pm 0.2\%$ , respectively) were significantly greater than the average of all other systems ( $39.8 \pm 0.3\%$ ), with hotspots mainly in regions with tropical and subtropical croplands (e.g., Southeastern Asia and Amazon Plain) for single rice, and North high-altitude areas for single wheat. The intrinsic variation in  $R_{\text{fallow}}$  for these cropping systems can also be found in the observations included in our dataset (Figure 1c). Single legumes, maize and other systems showed similar spatial variations in  $R_{\text{fallow}}$  as the area-weighted averages of all systems (Figure 2a).

### 3.3 | Attribution of the spatial variation in $R_{\text{fallow}}$

Soil pH was identified as the most important driver of spatial variation in  $R_{\text{fallow}}$  in 72% of the total global cropping area (Figure 3a). For all cropping systems other than single rice, soil pH was the most important driver in most ( $\geq 59\%$ ) of their individual global cropping area (Figure 3b-i). These results likely reflect that low

soil pH inhibit the activity of  $\text{N}_2\text{O}$  reductase in denitrification and reduce the precursor concentration of  $\text{N}_2\text{O}$  formation (i.e.,  $\text{NH}_2\text{OH}$  and  $\text{NO}_2^-$ ) in nitrification, thereby stimulating  $\text{N}_2\text{O}$  emissions (Barton et al., 2013; Qin et al., 2014; Russenes et al., 2016; Wang et al., 2021). Consistent with these findings, low soil pH values are associated with greater fallow-period  $\text{N}_2\text{O}$  emissions across the observations included in our dataset (Correlation coefficient =  $-0.31$ ,  $p < .001$ ), leading to the increasing  $R_{\text{fallow}}$  values with decreasing soil pH. This is probably because lower temperature during the fallow period (e.g., winter season) further inhibits the  $\text{N}_2\text{O}$  reductase activity (Qin et al., 2014). Additionally, lower pH levels are correlated with more precipitation in fallow periods in our dataset (Correlation coefficient =  $-0.1$ ,  $p < .05$ ). High precipitation rates may stimulate fallow-period  $\text{N}_2\text{O}$  emissions when low soil water content is the limiting factor for  $\text{N}_2\text{O}$  emissions especially in arid areas (Shang et al., 2020). Since about 50% of global arable soils are acidic, liming has been suggested as a potential practice to increase crop yield (Dai et al., 2017; Wang et al., 2021). In this case, soil liming can decrease the contribution



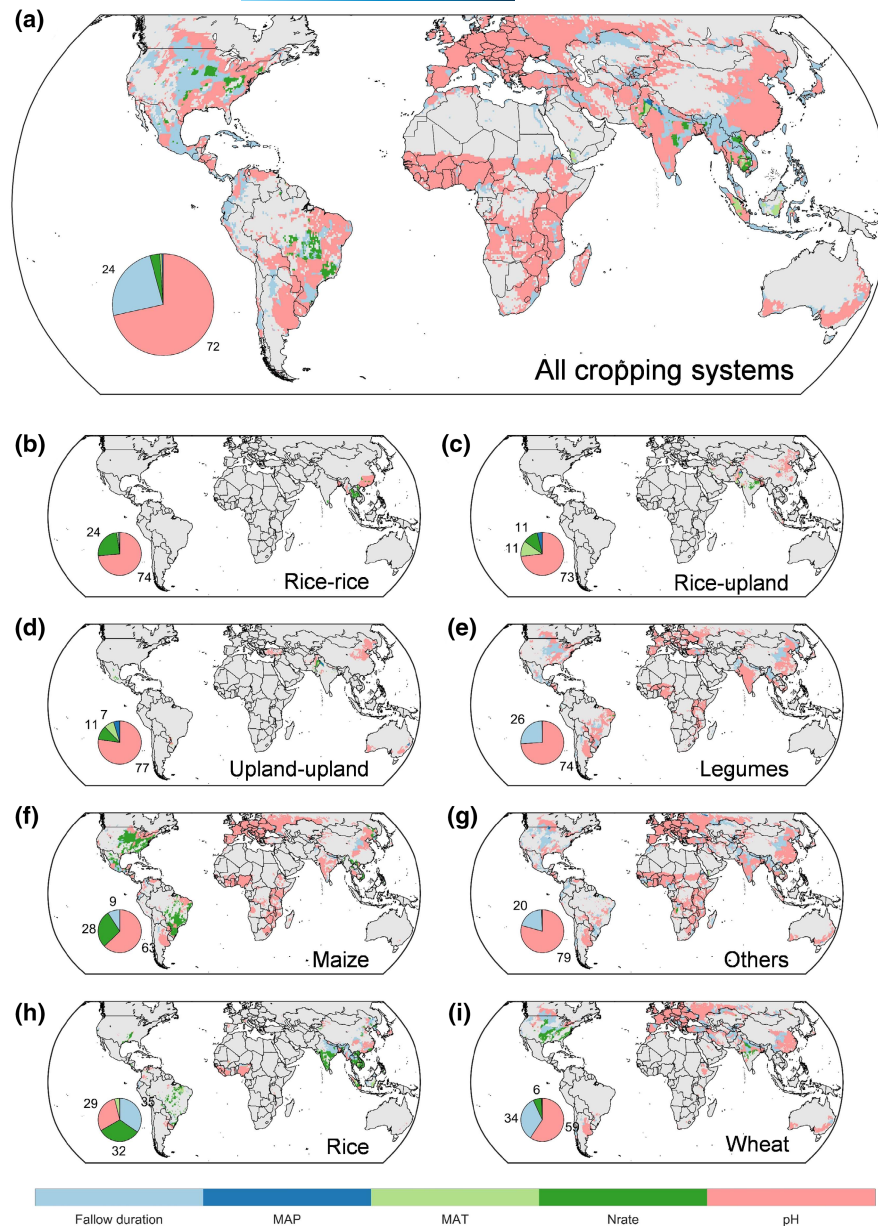


**FIGURE 3** Distribution of dominant drivers regulating variation in  $R_{\text{fallow}}$ . (a) Ratios weighted by areas of different cropping systems, including the double (rice-rice (b), rice-upland crops (c) and upland-upland crops (d)) and single (legumes (e), maize (f), others (g), rice (h) and wheat (i)). The dominant driver is defined as the factor with the largest absolute value of the partial correlation coefficient ( $\rho_{\text{par}}$ ) in each grid cell, where  $\rho_{\text{par}}$  between  $R_{\text{fallow}}$  and predictors is done for  $3.75^\circ \times 3.75^\circ$  moving windows. Significant correlations ( $p < .05$ ) are shown. Values are shown only where the proportion of harvested area within the grid cell is greater than 0.5%. The inset pie plots represent the ratio (%) of harvested areas for which  $R_{\text{fallow}}$  variation is regulated by the dominant drivers. MAP, mean annual precipitation; MAT, mean annual temperature; Nrate, N application rate. Map lines delineate study areas and do not necessarily depict accepted national boundaries.

of fallow period to whole-year  $\text{N}_2\text{O}$  emissions in severely acidic area ( $\text{pH} < 5.5$ ) concentrated in Eastern United States, Northern Germany and Poland, Southern China and Southeastern Brazil (Wang et al., 2021) and hence influence the growing-season to whole-year  $\text{N}_2\text{O}$  correction factors for these areas.

Fallow duration was identified as the most important driver for  $R_{\text{fallow}}$  in single rice cropping systems and the second most important factor in most other single cropping systems accounting for 20%–34% of the variations in their cropping areas, especially in North America, Northern South America and Northern China (Figure 3e–i). A longer fallow period directly results in more  $\text{N}_2\text{O}$  emissions during this fallow period, confirmed by the positive relationships between duration and  $R_{\text{fallow}}$  across our dataset (Figure 1f). Compared with double cropping systems, single cropping systems generally have a longer and more variable fallow period that is constrained by local climates. For example, single rice systems have a longer fallow period

(1–2 months more) in Northeastern compared with Southern China. These single rice systems in Southern China are usually transformed from double rice systems due to labour shortage (Han et al., 2022), although the light, temperature and rainfall there are favourable for double rice growth. In contrast, the double cropping systems, such as maize-wheat and rice-wheat in Turkey, Northern and Eastern China, generally have a much shorter fallow period, ranging from 2 to 3 months. This relatively short fallow period likely explains the negligible effect of fallow duration on the spatial variation in  $R_{\text{fallow}}$  for double cropping systems (Figure 3b–d).

The results indicate N application rate was the most important driver in 11%–32% of global cropping areas for both double cropping systems and single rice and maize systems (Figure 3).  $R_{\text{fallow}}$  estimated generally decreases with increased N application rates (Figure 1e). This is because fertilizer-induced  $\text{N}_2\text{O}$  emissions mostly occurred during the crop growing seasons when crops need intensive

N fertilizer inputs, with limited fertilizer N residues for N<sub>2</sub>O emissions during the fallow seasons. MAT was identified as a key factor only in limited areas for double upland crops. However, it emerged as the dominant driver for the variation weighted by cropping systems in Africa, South America and Southeast Asia.

### 3.4 | Implications for updating N<sub>2</sub>O emission inventories

We converted N<sub>2</sub>O emissions during the growing season to cover the whole-year emissions (Table 2), based on the estimated area-weighted R<sub>fallow</sub>, the growing-season dominated default EFs from the IPCC Tier 1 method and our high-resolution cropping-system-specific N application rate developed in this study. Estimated global fertilizer N-induced cropland N<sub>2</sub>O emissions in 2000 substantially increased from 1.0 to 2.1 Tg N, implying a global R<sub>fallow</sub> of ~53%. Emission hotspots were located in several countries such as China, France, Germany, the United States and the UK (Figure S8). Accordingly, the EF more than doubled from 0.9% (based on IPCC Tier 1 defaults of 0.4% for paddy rice and 1.0% for upland crops) to 1.9% (0.6% for paddy rice and 2.1% for upland crops). High-adjusted EFs (i.e., >2%) were concentrated in regions like Brazil, Middle Africa, Southeast Asia and high-altitude regions in Europe (Figure 4a). The adjusted global EF is more than twice as large as those from EF-based models based on growing-season N<sub>2</sub>O observations (Table 2) and is consistent with results from an ensemble of process-based models (1.8%, 1.2%–2.3%; Tian et al., 2020) and a recent top-down inversion model (2.3%; Thompson et al., 2019). The process-based models considered the legacy effect from historical soil N accumulation (Tian et al., 2019, 2020), which is the main source of N<sub>2</sub>O emissions during the fallow period without fertilization. Since the inversion model estimates EFs based on observed changes in atmospheric N<sub>2</sub>O concentrations, it accounts for both direct and indirect emissions. Indirect emissions were not included in our study but

account for about one-third of total cropland N<sub>2</sub>O emissions (Harris et al., 2022). Comparing our findings with the IPCC Tier 1 defaults, significant increases in EFs were found in Russia, Myanmar and some areas dominated by acidic soils and single cropping systems (e.g., wheat and maize) (Figure 4b), while the increase was trivial in East India and Pakistan, probably due to the vast expansion of double cropping systems (e.g., rice-upland crops and upland-upland crops) with shorter fallow durations (Sacks et al., 2010; Waha et al., 2020), alongside the prevalence of alkaline soils in Pakistan. The consistency between the estimates of our corrected EF-based model and other independent models strongly suggests that most of the discrepancies between the models were caused by the omission of fallow-period N<sub>2</sub>O emissions. Our findings are also in alignment with previous findings that the global EF for cropland N<sub>2</sub>O emissions is significantly higher than the IPCC default (Thompson et al., 2019; Tian et al., 2020). Thus, to improve estimates of N<sub>2</sub>O inventories, we suggest that fallow-period N<sub>2</sub>O emissions should be included in the EF-based models. For the datasets reporting growing-season N<sub>2</sub>O emissions only, without considering fallow-period emissions, they should not be further considered in the calculation of IPCC N<sub>2</sub>O EFs. IPCC should update the relevant EFs.

### 3.5 | Limitations and future perspective

Although our approach considers the influences of various important factors, some limitations should be noted. First, to improve our estimation for various cropping systems (e.g., double rice-rice, single rice and single wheat systems), more field measurements of fallow-period N<sub>2</sub>O emissions are needed for double rice-upland crops, upland-upland crops and single legume systems. About 81% of the observations are based on averaged or intensified sampling intervals of no more than 7 days during fallow period (Text S2); however, future field studies should ensure frequent fallow-period measurements, especially during N<sub>2</sub>O peak-flux periods (e.g.,

TABLE 2 Cropland fertilizer-induced N<sub>2</sub>O emissions and emission factor from main approaches.

Methodology	Year	Emission (Tg N)	EF (%)	Citation
This study	2000	2.1	1.9	This study
Emission factor-based model	2000	1.0–1.4	0.9–1.0	
FAO <sup>a</sup>	2000	1.3	0.9	FAOSTAT (2022)
EDGAR <sup>a</sup>	2000	1.5	0.9	Crippa et al. (2021)
GAINS <sup>a</sup>	2000	1.4	0.9	Winiwarter et al. (2018)
SRNM	2000	1.1	1.0	Wang et al. (2020)
LME	2000	1.0	0.9	Cui et al. (2021)
Process-based model ensemble	2000s	2 (1.3–3.4) <sup>b</sup>	1.8 (1.2–2.3)	Tian et al. (2020)
Atmospheric inversion <sup>c</sup>	1998–2016	–	2.3 ± 0.6	Thompson et al. (2019)

<sup>a</sup>FAOSTAT and GAINS were normalized by removing the contribution from synthetic fertilizers applied to pasture; the EDGAR version 4.3.2 by excluding the contributions from synthetic fertilizers applied to pasture and soil mineralization.

<sup>b</sup>The emission from the ensemble of process-based models includes cropland and pasture N<sub>2</sub>O emissions.

<sup>c</sup>The inversion model includes direct and indirect N<sub>2</sub>O emissions.



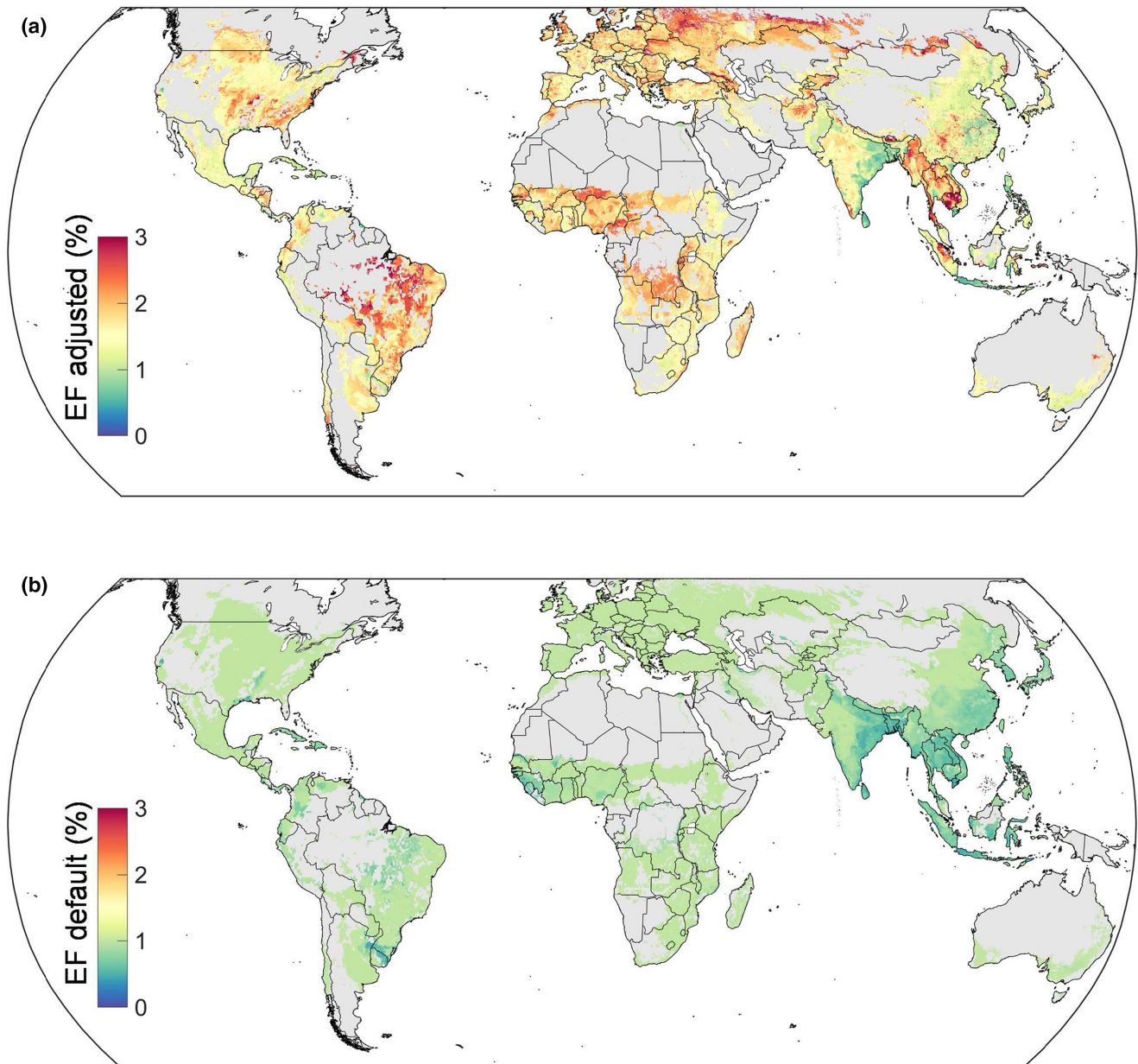


**FIGURE 4** Spatial variation of cropland N<sub>2</sub>O EF estimated in this study (a) and based on IPCC Tier 1 EF defaults (b). The  $R_{\text{fallow}}$  used was the area-weighted of all cropping systems. Map lines delineate study areas and do not necessarily depict accepted national boundaries.

spring thawing and tillage) to improve data reliability. Second, site-specific microscale variables were less recorded and their effects on local N<sub>2</sub>O emissions were not fully quantified due to limited understanding of the mechanisms of microbial N<sub>2</sub>O productions (Cui et al., 2021; Kravchenko et al., 2017). These can lead to some uncertainties in the global simulation; however, the fixed effect in the model developed explained more variation in  $R_{\text{fallow}}$  than the random effect (represented by site identity) did. Other uncertainties come from recently introduced or highly localized practices in fallow periods, such as winter cover cropping, tillage and continuous flooding for water storage in hilly rice paddies. Although tillage showed an insignificant impact on growing-season or whole-year N<sub>2</sub>O emissions based on meta-analyses (Shang et al., 2021; van

Kessel et al., 2013), it can increase fallow-period N<sub>2</sub>O emissions due to the favourable soil aeration and water content for N<sub>2</sub>O productions in field experiments (Mosier et al., 2006; Zhang et al., 2016). Similarly, the return of crop residue or green manure can increase fallow-period N<sub>2</sub>O emissions in the fields through providing more C and N substrates for nitrification and denitrification processes (Li et al., 2021; Liu et al., 2016). As indicated in the field studies above, fallow tillage and return of crop residue or green manure generally have a more positive impact on fallow period over growing-season N<sub>2</sub>O emissions and hence increase the value of  $R_{\text{fallow}}$ . However, these effects may vary with time (e.g., beginning or end of fallow period) and type of practice (e.g., straw mulching or incorporation and residue composition), which needs more information and

deserves further investigation. Constrained by the availability of crop-specific spatial data, the global  $R_{\text{fallow}}$  was estimated using the spatial distribution of cropping systems in 2000. Some single cropping systems have evolved to double cropping systems and vice versa over the last 20 years (Han et al., 2022), which might slightly affect the contribution of fallow-period emission in recent years. However, our model is not restricted to specific years and sites, and it can be applied universally based on essential factors such as soil properties and management practices, regardless of time and space.

$\text{N}_2\text{O}$  emissions in fallow period have been ignored when calculating the whole-year emissions for decades, even though this will lead to the underestimation of  $\text{N}_2\text{O}$  emission inventories. One major objective of our study was to understand the degree to which cropland  $\text{N}_2\text{O}$  emissions have been underestimated in the EF-based models. Here, we demonstrate that the inclusion of fallow-period  $\text{N}_2\text{O}$  emissions is crucial for compiling accurate cropland whole-year  $\text{N}_2\text{O}$  emission inventories. In particular, single wheat and other single cropping systems dominate most global fallow emissions, contributing up to 89% of their whole-year emissions. Overall, our estimates of the global average EF more than doubled from 0.9% to 1.9% when the emissions during the fallow periods were considered, with variations in  $R_{\text{fallow}}$  mainly driven by soil pH and management practices (i.e., cropping system type, N fertilizer application rate and fallow duration). Current EF-based models systemically underestimate  $\text{N}_2\text{O}$  fluxes without the corresponding adjustment for the fallow period. Additionally, process-based models are barely capable of calibrating and validating against the measurements of fallow-period  $\text{N}_2\text{O}$  emissions, due to the limitation of available fallow emission measurements. Hence, a sharing platform of global fallow-period  $\text{N}_2\text{O}$  emission measurements is needed to gather more comprehensive data on fallow-period  $\text{N}_2\text{O}$  emissions. Further research is required to check whether historical trends and future projections of national cropland  $\text{N}_2\text{O}$  emissions would be impacted by the inclusion of fallow period. Additionally, research on potential mitigation practices specific to reducing  $\text{N}_2\text{O}$  emissions during fallow periods is needed, especially for single or rice-related cropping systems. Overall, our study extends our understanding of the contribution of fallow-period  $\text{N}_2\text{O}$  emissions—the global magnitude, spatial variation and their environmental and anthropogenic drivers. We hope our approach can be used to improve future  $\text{N}_2\text{O}$  inventories and to inform mitigation efforts to reduce cropland  $\text{N}_2\text{O}$  emissions.

## AUTHOR CONTRIBUTIONS

**Ziyin Shang:** Conceptualization; data curation; formal analysis; funding acquisition; investigation; methodology; visualization; writing – original draft. **Xiaoqing Cui:** Methodology; visualization; writing – original draft. **Kees Jan van Groenigen:** Conceptualization; resources; writing – review and editing. **Matthias Kuhnert:** Conceptualization; resources; writing – review and editing. **Mohamed Abdalla:** Conceptualization; resources; writing – review and editing. **Jiafa Luo:** Conceptualization; resources; writing – review and editing. **Weijian Zhang:** Conceptualization; resources; writing – review and editing.

**Zhenwei Song:** Conceptualization; resources; writing – review and editing. **Yu Jiang:** Conceptualization; resources; writing – review and editing. **Pete Smith:** Conceptualization; resources; writing – review and editing. **Feng Zhou:** Conceptualization; funding acquisition; project administration; writing – review and editing.

## ACKNOWLEDGEMENTS

This study was supported by the National Natural Science Foundation of China (42225102, 42361144876, 42301059, 32172129 and 42207378), The Youth Innovation Program of Chinese Academy of Agricultural Sciences (No. Y2023QC02), the National Key Research and Development Program of China (2021YFD1700801 and 2022YFD2300400) and Technology Research System-Green Manure (Grant No. CARS-22-G-16).

## CONFLICT OF INTEREST STATEMENT

The authors declare no conflicts of interest.

## DATA AVAILABILITY STATEMENT

The data that support the findings of this study are openly available in figshare at <http://doi.org/10.6084/m9.figshare.24941466> and <http://doi.org/10.6084/m9.figshare.24945633>.

## ORCID

Ziyin Shang  <https://orcid.org/0000-0001-8840-0380>  
 Xiaoqing Cui  <https://orcid.org/0000-0002-1970-5145>  
 Kees Jan van Groenigen  <https://orcid.org/0000-0002-9165-3925>  
 Matthias Kuhnert  <https://orcid.org/0000-0003-3284-2133>  
 Mohamed Abdalla  <https://orcid.org/0000-0001-8403-327X>  
 Jiafa Luo  <https://orcid.org/0000-0001-6198-6887>  
 Weijian Zhang  <https://orcid.org/0009-0006-9043-687X>  
 Zhenwei Song  <https://orcid.org/0000-0001-9057-2157>  
 Yu Jiang  <https://orcid.org/0000-0002-4241-1858>  
 Pete Smith  <https://orcid.org/0000-0002-3784-1124>  
 Feng Zhou  <https://orcid.org/0000-0001-6122-0611>

## REFERENCES

- Adalbieke, W., Cui, X. Q., Cai, H. W., You, L. Z., & Feng, Z. (2023). Global crop-specific nitrogen fertilization dataset in 1961–2020. *Scientific Data*, 10, 617. <https://doi.org/10.1038/s41597-023-02526-z>
- Barton, L., Gleeson, D. B., Maccarone, L. D., Zúñiga, L. P., & Murphy, D. V. (2013). Is liming soil a strategy for mitigating nitrous oxide emissions from semi-arid soils? *Soil Biology and Biochemistry*, 62, 28–35. <https://doi.org/10.1016/j.soilbio.2013.02.014>
- Beer, C., Reichstein, M., Tomelleri, E., Ciais, P., Jung, M., Carvalhais, N., Rödenbeck, C., Arain, M. A., Baldocchi, D., Bonan, G. B., Bondeau, A., Cescatti, A., Lasslop, G., Lindroth, A., Lomas, M., Luysaert, S., Margolis, H., Oleson, K. W., Rouspard, O., ... Papale, D. (2010). Terrestrial gross carbon dioxide uptake: Global distribution and covariation with climate. *Science*, 329(5993), 834–838. <https://doi.org/10.1126/science.1184984>
- Bo, Y., Jägermeyr, J., Yin, Z., Jiang, Y., Xu, J. Z., Liang, H., & Zhou, F. (2022). Global benefits of non-continuous flooding to reduce greenhouse gases and irrigation water use without rice yield penalty. *Global Change Biology*, 28(11), 3636–3650. <https://doi.org/10.1111/gcb.16132>

- Bouwman, A. F., Beusen, A. H. W., Griffioen, J., Van Groenigen, J. W., Hefting, M. M., Oenema, O., Van Puijenbroek, P., Seitzinger, S., Slomp, C. P., & Stehfest, E. (2013). Global trends and uncertainties in terrestrial denitrification and N<sub>2</sub>O emissions. *Philosophical Transactions of the Royal Society B: Biological Sciences*, 368, 20130112. <https://doi.org/10.1098/rstb.2013.0112>
- Butterbach-Bahl, K., Baggs, E. M., Dannenmann, M., Kiese, R., & Zechmeister-Boltenstern, S. (2013). Nitrous oxide emissions from soils: How well do we understand the processes and their controls? *Philosophical Transactions of the Royal Society B: Biological Sciences*, 368, 20130122. <https://doi.org/10.1098/rstb.2013.0122>
- Crippa, M., Guizzardi, D., Solazzo, E., Muntean, M., Schaaf, E., Monforti-Ferrario, F., Banja, M., Olivier, J. G. J., Grassi, G., Rossi, S., & Vignati, E. (2021). *GHG emissions of all world countries—2021 report*. Publications Office of the European Union. <https://doi.org/10.2760/173513>
- Cui, X. Q., Zhou, F., Ciais, P., Davidson, E. A., Tubiello, F. N., Niu, X. Y., Ju, X. T., Canadell, J. G., Bouwman, A. F., Jackson, R. B., Mueller, N. D., Zheng, X. H., Kanter, D. R., Tian, H. Q., Adalibieke, W., Bo, Y., Wang, Q. H., Zhan, X. Y., & Zhu, D. Q. (2021). Global mapping of crop-specific emission factors highlights hotspots of nitrous oxide mitigation. *Nature Food*, 2, 886–893. <https://doi.org/10.1038/s43016-021-00384-9>
- Dai, Z., Zhang, X., Tang, C., Muhammad, N., Wu, J., Brookes, P. C., & Xu, J. (2017). Potential role of biochars in decreasing soil acidification—A critical review. *Science of the Total Environment*, 581–582, 601–611. <https://doi.org/10.1016/j.scitotenv.2016.12.169>
- Deng, Z., Ciais, P., Tzompa-Sosa, Z. A., Saunio, M., Qiu, C., Tan, C., Sun, T., Ke, P., Cui, Y., Tanaka, K., Lin, X., Thompson, R. L., Tian, H., Yao, Y., Huang, Y., Lauerwald, R., Jain, A. K., Xu, X., Bastos, A., ... Chevallier, F. (2022). Comparing national greenhouse gas budgets reported in UNFCCC inventories against atmospheric inversions. *Earth System Science Data*, 14, 1639–1675. <https://doi.org/10.5194/essd-14-1639-2022>
- Ekwunife, K. C., Madramootoo, C. A., & Abbasi, N. A. (2022). Assessing the impacts of tillage, cover crops, nitrification, and urease inhibitors on nitrous oxide emissions over winter and early spring. *Biology and Fertility of Soils*, 58, 195–206. <https://doi.org/10.1007/s00374-021-01605-w>
- FAO Food and Agricultural Organization of the United Nations. (2022). *FAOSTAT data*. <http://www.fao.org/faostat/en/#data/RFN> (Fertilizers by Nutrient); <http://www.fao.org/faostat/en/#data/EMN> (Live-stock Manure); <http://www.fao.org/faostat/en/#data/GA> (Crop Residues); <http://www.fao.org/faostat/en/#data/GT> (Emissions-Agriculture)
- Han, J. C., Zhang, Z., Luo, Y. C., Cao, J., Zhang, L. L., Zhuang, H. M., Cheng, F., Zhang, J., & Tao, F. L. (2022). Annual paddy rice planting area and cropping intensity datasets and their dynamics in the Asian monsoon region from 2000 to 2020. *Agricultural Systems*, 200, 103437. <https://doi.org/10.1016/j.agsy.2022.103437>
- Harris, E., Yu, L., Wang, Y. P., Mohn, J., Henne, S., Bai, E., Barthel, M., Bauters, M., Boeckx, P., Dorich, C., Farrell, M., Krummel, P. B., Loh, Z. M., Reichstein, M., Six, J., Steinbacher, M., Wells, N. S., Bahn, M., & Rayner, P. (2022). Warming and redistribution of nitrogen inputs drive an increase in terrestrial nitrous oxide emission factor. *Nature Communications*, 13, 4310. <https://doi.org/10.1038/s41467-022-32001-z>
- IPCC. (2006). *2006 guidelines for national greenhouse gas inventories*. IPCC.
- Kravchenko, A. N., Toosi, E. R., Guber, A. K., Ostrom, N. E., Yu, J., Azeem, K., Rivers, M. L., & Robertson, G. P. (2017). Hotspots of soil N<sub>2</sub>O emission enhanced through water absorption by plant residue. *Nature Geoscience*, 10(7), 496–500. <https://doi.org/10.1038/Ngeo2963>
- Li, J., Wang, S., Shi, Y. L., Zhang, L. L., & Wu, Z. J. (2021). Do fallow season cover crops increase N<sub>2</sub>O or CH<sub>4</sub> emission from paddy soils in the mono-rice cropping system? *Agronomy-Basel*, 11(2), 199. <https://doi.org/10.3390/agronomy11020199>
- Liu, W., Hussain, S., Wu, L. S., Qin, Z. G., Li, X. K., Lu, J. W., Khan, F., Cao, W. D., & Geng, M. J. (2016). Greenhouse gas emissions, soil quality, and crop productivity from a mono-rice cultivation system as influenced by fallow season straw management. *Environmental Science and Pollution Research*, 23(1), 315–328. <https://doi.org/10.1007/s11356-015-5227-7>
- Malakouti, S. M. (2023). Improving the prediction of wind speed and power production of SCADA system with ensemble method and 10-fold cross-validation. *Case Studies in Chemical and Environmental Engineering*, 8, 100351. <https://doi.org/10.1016/j.csee.2023.100351>
- Monfreda, C., Ramankutty, N., & Foley, J. A. (2008). Farming the planet: 2. Geographic distribution of crop areas, yields, physiological types, and net primary production in the year 2000. *Global Biogeochemical Cycles*, 22(1), Gb1022. <https://doi.org/10.1029/2007gb002947>
- Mosier, A. R., Halvorson, A. D., Reule, C. A., & Liu, X. J. J. (2006). Net global warming potential and greenhouse gas intensity in irrigated cropping systems in northeastern Colorado. *Journal of Environmental Quality*, 35(4), 1584–1598. <https://doi.org/10.2134/jeq2005.0232>
- Pelster, D. E., Thiagarajan, A., Liang, C., Chantigny, M. H., Wagner-Riddle, C., Congreves, K., Lemke, R., Glenn, A., Tenuta, M., Hernandez-Ramirez, G., Bittman, S., Hunt, D., Owens, J., & MacDonald, D. (2022). Ratio of non-growing season to growing season N<sub>2</sub>O emissions in Canadian croplands: An update to national inventory methodology. *Canadian Journal of Soil Science*, 103, 344–352. <https://doi.org/10.1139/cjss-2022-0101>
- Peng, S. S., Piao, S. L., Ciais, P., Myneni, R. B., Chen, A. P., Chevallier, F., Dolman, A. J., Janssens, I. A., Peñuelas, J., Zhang, G. X., Vicca, S., Wan, S. Q., Wang, S. P., & Zeng, H. (2013). Asymmetric effects of daytime and night-time warming on northern hemisphere vegetation. *Nature*, 501(7465), 88–92. <https://doi.org/10.1038/nature12434>
- Philibert, A., Loyce, C., & Makowski, D. (2012). Quantifying uncertainties in N<sub>2</sub>O emission due to N fertilizer application in cultivated areas. *PLoS ONE*, 7(11), e50950. <https://doi.org/10.1371/journal.pone.0050950>
- Qin, S. P., Yuan, H. J., Hu, C. S., Oenema, O., Zhang, Y. M., & Li, X. X. (2014). Determination of potential N<sub>2</sub>O-reductase activity in soil. *Soil Biology & Biochemistry*, 70, 205–210. <https://doi.org/10.1016/j.soilbio.2013.12.027>
- Ravishankara, A., Daniel, J. S., & Portmann, R. W. (2009). Nitrous oxide (N<sub>2</sub>O): The dominant ozone-depleting substance emitted in the 21st century. *Science*, 326, 123–125. <https://doi.org/10.1126/science.1176985>
- Russenes, A. L., Korsae, A., Bakken, L. R., & Dorsch, P. (2016). Spatial variation in soil pH controls off-season N<sub>2</sub>O emission in an agricultural soil. *Soil Biology & Biochemistry*, 99, 36–46. <https://doi.org/10.1016/j.soilbio.2016.04.019>
- Sacks, W. J., Deryng, D., Foley, J. A., & Ramankutty, N. (2010). Crop planting dates: An analysis of global patterns. *Global Ecology and Biogeography*, 19, 607–620. <https://doi.org/10.1111/j.1466-8238.2010.00551.x>
- Shang, Z. Y., Abdalla, M., Kuhnert, M., Albanito, F., Zhou, F., Xia, L. L., & Smith, P. (2020). Measurement of N<sub>2</sub>O emissions over the whole year is necessary for estimating reliable emission factors. *Environmental Pollution*, 259, 113864. <https://doi.org/10.1016/j.envpol.2019.113864>
- Shang, Z. Y., Abdalla, M., Xia, L. L., Zhou, F., Sun, W. J., & Smith, P. (2021). Can cropland management practices lower net greenhouse emissions without compromising yield? *Global Change Biology*, 27(19), 4657–4670. <https://doi.org/10.1111/gcb.15796>
- Thompson, R. L., Lassaletta, L., Patra, P. K., Wilson, C., Wells, K. C., Gressent, A., Koffi, E. N., Chipperfield, M. P., Winiwarter, W., Davidson, E. A., Tian, H., & Canadell, J. G. (2019). Acceleration of global N<sub>2</sub>O emissions seen from two decades of atmospheric



- inversion. *Nature Climate Change*, 9, 993–998. <https://doi.org/10.1038/s41558-019-0613-7>
- Tian, H. Q., Xu, R. T., Canadell, J. G., Thompson, R. L., Winiwarter, W., Suntharalingam, P., Davidson, E. A., Ciais, P., Jackson, R. B., Janssens-Maenhout, G., Prather, M. J., Regnier, P., Pan, N. Q., Pan, S. F., Peters, G. P., Shi, H., Tubiello, F. N., Zaehle, S., Zhou, F., ... Yao, Y. Z. (2020). A comprehensive quantification of global nitrous oxide sources and sinks. *Nature*, 586, 248–256. <https://doi.org/10.1038/s41586-020-2780-0>
- Tian, H. Q., Yang, J., Xu, R. T., Lu, C. Q., Canadell, J. G., Davidson, E. A., Jackson, R. B., Arneeth, A., Chang, J. F., Ciais, P., Gerber, S., Ito, A., Joos, F., Lienert, S., Messina, P., Olin, S., Pan, S. F., Peng, C. H., Saikawa, E., ... Zhang, B. W. (2019). Global soil nitrous oxide emissions since the preindustrial era estimated by an ensemble of terrestrial biosphere models: Magnitude, attribution, and uncertainty. *Global Change Biology*, 25, 640–659. <https://doi.org/10.1111/gcb.14514>
- van den Hoogen, J., Geisen, S., Routh, D., Ferris, H., Traunspurger, W., Wardle, D. A., de Goede, R. G. M., Adams, B. J., Ahmad, W., Andriuzzi, W. S., Bardgett, R. D., Bonkowski, M., Campos-Herrera, R., Cares, J. E., Caruso, T., Caixeta, L. D., Chen, X. Y., Costa, S. R., Creamer, R., ... Crowther, T. W. (2019). Soil nematode abundance and functional group composition at a global scale. *Nature*, 572(7768), 194–198. <https://doi.org/10.1038/s41586-019-1418-6>
- van Kessel, C., Venterea, R., Six, J., Adviento-Borbe, M. A., Linquist, B., & van Groenigen, K. J. (2013). Climate, duration, and N placement determine N<sub>2</sub>O emissions in reduced tillage systems: A meta-analysis. *Global Change Biology*, 19(1), 33–44. <https://doi.org/10.1111/j.1365-2486.2012.02779.x>
- Viscarra Rossel, R. A., Lee, J., Behrens, T., Luo, Z., Baldock, J., & Richards, A. (2019). Continental-scale soil carbon composition and vulnerability modulated by regional environmental controls. *Nature Geoscience*, 12(7), 547–552. <https://doi.org/10.1038/s41561-019-0373-z>
- Waha, K., Dietrich, J. P., Portmann, F. T., Siebert, S., Thornton, P. K., Bondeau, A., & Herrero, M. (2020). Multiple cropping systems of the world and the potential for increasing cropping intensity. *Global Environmental Change-Human and Policy Dimensions*, 64, 102131. <https://doi.org/10.1016/j.gloenvcha.2020.102131>
- Wang, Q., Zhou, F., Shang, Z., Ciais, P., Winiwarter, W., Jackson, R. B., Tubiello, F. N., Janssens-Maenhout, G., Tian, H., Cui, X., Canadell, J. G., Piao, S., & Tao, S. (2020). Data-driven estimates of global nitrous oxide emissions from croplands. *National Science Review*, 7, 441–452. <https://doi.org/10.1093/nsr/nwz087>
- Wang, Y., Yao, Z. S., Zhan, Y., Zheng, X. H., Zhou, M. H., Yan, G. X., Wang, L., Werner, C., & Butterbach-Bahl, K. (2021). Potential benefits of liming to acid soils on climate change mitigation and food security. *Global Change Biology*, 27(12), 2807–2821. <https://doi.org/10.1111/gcb.15607>
- Winiwarter, W., Hoglund-Isaksson, L., Klimont, Z., Schoepp, W., & Amann, M. (2018). Technical opportunities to reduce global anthropogenic emissions of nitrous oxide. *Environmental Research Letters*, 13, 014011. <https://doi.org/10.1088/1748-9326/aa9ec9>
- Yang, Y. F., Liu, L. C., Zhou, W., Guan, K. Y., Tang, J. Y., Kim, T., Grant, R. F., Peng, B., Zhu, P., Li, Z. Y., Griffis, T. J., & Jin, Z. N. (2023). Distinct driving mechanisms of non-growing season N<sub>2</sub>O emissions call for spatial-specific mitigation strategies in the US Midwest. *Agricultural and Forest Meteorology*, 335, 109457. <https://doi.org/10.1016/j.agrformet.2023.109457>
- Zhang, G. B., Yu, H. Y., Fan, X. F., Yang, Y. T., Ma, J., & Xu, H. (2016). Drainage and tillage practices in the winter fallow season mitigate CH<sub>4</sub> and N<sub>2</sub>O emissions from a double-rice field in China. *Atmospheric Chemistry and Physics*, 16(18), 11853–11866. <https://doi.org/10.5194/acp-16-11853-2016>
- ## DATA SOURCES
- Abao, E. B., Bronson, K. F., Wassmann, R., & Singh, U. (2000). Simultaneous records of methane and nitrous oxide emissions in rice-based cropping systems under rainfed conditions. *Nutrient Cycling in Agroecosystems*, 58(1–3), 131–139. <https://doi.org/10.1023/A:1009842502608>
- Adviento-Borbe, M. A., Pittelkow, C. M., Anders, M., van Kessel, C., Hill, J. E., McClung, A. M., Six, J., & Linquist, B. A. (2013). Optimal fertilizer nitrogen rates and yield-scaled global warming potential in drill seeded rice. *Journal of Environmental Quality*, 42(6), 1623–1634. <https://doi.org/10.2134/jeq2013.05.0167>
- Aita, C., Schirrmann, J., Pujol, S. B., Giacomini, S. J., Rochette, P., Angers, D. A., Chantigny, M. H., Gonzatto, R., Giacomini, D. A., & Doneda, A. (2015). Reducing nitrous oxide emissions from a maize-wheat sequence by decreasing soil nitrate concentration: Effects of split application of pig slurry and dicyandiamide. *European Journal of Soil Science*, 66(2), 359–368. <https://doi.org/10.1111/ejss.12181>
- Baral, K. R., Jayasundara, S., Brown, S. E., & Wagner-Riddle, C. (2022). Long-term variability in N<sub>2</sub>O emissions and emission factors for corn and soybeans induced by weather and management at a cold climate site. *Science of the Total Environment*, 815, 152744. <https://doi.org/10.1016/j.scitotenv.2021.152744>
- Barton, L., Kiese, R., Gatter, D., Butterbach-Bahl, K., Buck, R., Hinz, C., & Murphy, D. V. (2008). Nitrous oxide emissions from a cropped soil in a semi-arid climate. *Global Change Biology*, 14(1), 177–192. <https://doi.org/10.1111/j.1365-2486.2007.01474.x>
- Barton, L., Murphy, D. V., Kiese, R., & Butterbach-Bahl, K. (2010). Soil nitrous oxide and methane fluxes are low from a bioenergy crop (canola) grown in a semi-arid climate. *Global Change Biology*, 16(1), 1–15. <https://doi.org/10.1111/j.1365-2486.2009.01934.x>
- Chen, Y. D., Zhao, Y., Gao, D. J., Luo, X. F., Cui, T., Tong, Z. Q., & Wu, J. M. (2020). Effects of different rotation patterns of oil-rice on methane and nitrous oxide emissions in rice fields (in Chinese). *Environmental Sciences*, 41(10), 4701–4710. <https://doi.org/10.13227/j.hjhx.202002107>
- Chen, Z. M., Ding, W. X., Luo, Y. Q., Yu, H. Y., Xu, Y. H., Müller, C., Xu, X., & Zhu, T. B. (2014). Nitrous oxide emissions from cultivated black soil: A case study in Northeast China and global estimates using empirical model. *Global Biogeochemical Cycles*, 28(11), 1311–1326. <https://doi.org/10.1002/2014gb004871>
- Chen, Z. M., Li, Y., Xu, Y. H., Lam, S. K., Xia, L. L., Zhang, N., Castellano, M. J., & Ding, W. X. (2021). Spring thaw pulses decrease annual N<sub>2</sub>O emissions reductions by nitrification inhibitors from a seasonally frozen cropland. *Geoderma*, 403, 115310. <https://doi.org/10.1016/j.geoderma.2021.115310>
- Dalal, R. C., Gibson, I., Allen, D. E., & Menzies, N. W. (2010). Green waste compost reduces nitrous oxide emissions from feedlot manure applied to soil. *Agriculture Ecosystems & Environment*, 136(3–4), 273–281. <https://doi.org/10.1016/j.agee.2009.06.010>
- Dick, J., Kaya, B., Soutoura, M., Skiba, U., Smith, R., Niang, A., & Tabo, R. (2008). The contribution of agricultural practices to nitrous oxide emissions in semi-arid Mali. *Soil Use and Management*, 24(3), 292–301. <https://doi.org/10.1111/j.1475-2743.2008.00163.x>
- Ding, W. X., Cai, Y., Cai, Z. C., Yagi, K., & Zheng, X. H. (2007). Nitrous oxide emissions from an intensively cultivated maize-wheat rotation soil in the North China plain. *Science of the Total Environment*, 373(2–3), 501–511. <https://doi.org/10.1016/j.scitotenv.2006.12.026>
- Dungan, R. S., Leytem, A. B., Moore, A. D., Bjorneberg, D. L., Grace, P. R., Brunk, C., & Rowlands, D. W. (2023). Growing and non-growing season nitrous oxide emissions from a manured semi-arid cropland soil under irrigation. *Agriculture Ecosystems & Environment*, 348, 108413. <https://doi.org/10.1016/j.agee.2023.108413>
- Hou, X. L. (2012). *Study on soil carbon sequestration and emission mitigation under different fertilization* (in Chinese). Chinese Academy of Agricultural Sciences.
- Huérffano, X., Fuertes-Mendizábal, T., Duñabeitia, M. K., González-Murua, C., Estavillo, J. M., & Menéndez, S. (2015). Splitting the application of 3,4-dimethylpyrazole phosphate (DMPP): Influence on greenhouse gases emissions and wheat yield and quality under humid Mediterranean conditions. *European Journal of Agronomy*, 64, 47–57. <https://doi.org/10.1016/j.eja.2014.11.008>
- Kong, X. W., Liu, Y. L., Xiong, Z. Q., Ma, Y. C., Zhang, X. L., Qin, J. Q., & Tang, Q. Y. (2013). CH<sub>4</sub> and N<sub>2</sub>O emissions from double-rice field under different intensified cultivation patterns in Hunan Province (in Chinese). *Acta Scientiae Circumstantiae*, 9, 2612–2618. <https://doi.org/10.13671/j.hjxxb.2013.09.009>
- Lebender, U., Senbayram, M., Lammel, J., & Kuhlmann, H. (2014). Impact of mineral N fertilizer application rates on N<sub>2</sub>O emissions from arable soils under winter wheat. *Nutrient Cycling in Agroecosystems*, 100(1), 111–120. <https://doi.org/10.1007/s10705-014-9630-0>

- Li, J., Wang, S., Shi, Y. L., Zhang, L. L., & Wu, Z. J. (2021). Do fallow season cover crops increase N<sub>2</sub>O or CH<sub>4</sub> emission from paddy soils in the mono-rice cropping system? *Agronomy-Basel*, 11(2), 199. <https://doi.org/10.3390/agronomy11020199>
- Liu, L. T., Hu, C. S., Yang, P. P., Ju, Z. Q., Olesen, J. E., & Tang, J. W. (2016). Experimental warming-driven soil drying reduced N<sub>2</sub>O emissions from fertilized crop rotations of winter wheat-soybean/fallow, 2009–2014. *Agriculture Ecosystems & Environment*, 219, 71–82. <https://doi.org/10.1016/j.agee.2015.12.013>
- Liu, L. T., Knight, J. D., Lemke, R. L., & Farrell, R. E. (2021). Type of pulse crop included in a 2-year rotation with wheat affects total N<sub>2</sub>O loss and intensity. *Biology and Fertility of Soils*, 57(5), 699–713. <https://doi.org/10.1007/s00374-021-01562-4>
- Liu, W., Hussain, S., Wu, L. S., Qin, Z. G., Li, X. K., Lu, J. W., Khan, F., Cao, W. D., & Geng, M. J. (2016). Greenhouse gas emissions, soil quality, and crop productivity from a mono-rice cultivation system as influenced by fallow season straw management. *Environmental Science and Pollution Research*, 23(1), 315–328. <https://doi.org/10.1007/s11356-015-5227-7>
- Liu, Y. L. (2016). *Field studies on balance of greenhouse gas in annual double rice cropping systems under intenified cultivation patterns at different nitrogen rates* (in Chinese). Nanjing Agricultural University.
- Liu, Z. X. (2013). *Effects of tillage practices on greenhouse gases emissions from a purple soil under rice-rapeseed rotation system* (in Chinese). Southwest University.
- Lyu, X. D., Wang, T., Song, X. T., Zhao, C. Y., Rees, R. M., Liu, Z., Ju, X. T., & Siddique, K. H. M. (2021). Reducing N<sub>2</sub>O emissions with enhanced efficiency nitrogen fertilizers (EENFs) in a high-yielding spring maize system. *Environmental Pollution*, 273, 116422. <https://doi.org/10.1016/j.envpol.2020.116422>
- Mejjide, A., García-Torres, L., Arce, A., & Vallejo, A. (2009). Nitrogen oxide emissions affected by organic fertilization in a non-irrigated Mediterranean barley field. *Agriculture Ecosystems & Environment*, 132(1–2), 106–115. <https://doi.org/10.1016/j.agee.2009.03.005>
- Miao, S. J., Qiao, Y. F., Han, X. Z., Franco, R. B., & Burger, M. (2014). Frozen cropland soil in northeast China as source of N<sub>2</sub>O and CO<sub>2</sub> emissions. *PLoS ONE*, 9(12), e115761. <https://doi.org/10.1371/journal.pone.0115761>
- Mohamed, L. S. (2015). *Integrative effects of tillage and straw incorporation on rice yield and greenhouse gas emission from paddy field under double rice cropping system in Jiangxi Province* (in Chinese). Chinese Academy of Agricultural Sciences.
- Mosier, A. R., Halvorson, A. D., Reule, C. A., & Liu, X. J. (2006). Net global warming potential and greenhouse gas intensity in irrigated cropping systems in north-eastern Colorado. *Journal of Environmental Quality*, 35(4), 1584–1598. <https://doi.org/10.2134/jeq2005.0232>
- Naser, H. M., Nagata, O., Sultana, S., & Hatano, R. (2020). Carbon sequestration and contribution of CO<sub>2</sub>, CH<sub>4</sub> and N<sub>2</sub>O fluxes to global warming potential from paddy-fallow fields on mineral soil beneath peat in Central Hokkaido, Japan. *Agriculture-Basel*, 10(1), 6. <https://doi.org/10.3390/agriculture10010006>
- Nishimura, S., Sawamoto, T., Akiyama, H., Sudo, S., & Yagi, K. (2004). Methane and nitrous oxide emissions from a paddy field with Japanese conventional water management and fertilizer application. *Global Biogeochemical Cycles*, 18(2), Gb2017. <https://doi.org/10.1029/2003gb002207>
- Pittelkow, C. M., Adviento-Borbe, M. A., Hill, J. E., Six, J., van Kessel, C., & Linquist, B. A. (2013). Yield-scaled global warming potential of annual nitrous oxide and methane emissions from continuously flooded rice in response to nitrogen input. *Agriculture Ecosystems & Environment*, 177, 10–20. <https://doi.org/10.1016/j.agee.2013.05.011>
- Sanz-Cobena, A., Sánchez-Martín, L., García-Torres, L., & Vallejo, A. (2012). Gaseous emissions of N<sub>2</sub>O and NO and NO<sub>3</sub><sup>-</sup> leaching from urea applied with urease and nitrification inhibitors to a maize (*Zea mays*) crop. *Agriculture Ecosystems & Environment*, 149, 64–73. <https://doi.org/10.1016/j.agee.2011.12.016>
- Scheer, C., Rowlings, D. W., & Grace, P. R. (2016). Non-linear response of soil N<sub>2</sub>O emissions to nitrogen fertiliser in a cotton-fallow rotation in subtropical Australia. *Soil Research*, 54(5), 494–499. <https://doi.org/10.1071/Sr14328>
- Shang, Q. Y., Yang, X. X., Gao, C. M., Wu, P. P., Liu, J. J., Xu, Y. C., Shen, Q. R., Zou, J. W., & Guo, S. W. (2011). Net annual global warming potential and greenhouse gas intensity in Chinese double rice-cropping systems: A 3-year field measurement in long-term fertilizer experiments. *Global Change Biology*, 17(6), 2196–2210. <https://doi.org/10.1111/j.1365-2486.2010.02374.x>
- Shi, J. L. (2018). *Effect of plastic film mulching on greenhouse gases emission from a rice-rapeseed rotation cropland and its mitigation measures* (in Chinese). Southwest University.
- Su, M. M. (2016). *Greenhouse gases emissions and net global warming potential in croplands as affected by different rotation systems and nitrogen management in Sichuan Basin* (in Chinese). China Agricultural University.
- Su, S. (2018). *Effects of the paddy multiple cropping pattern on the greenhouse gas emission and soil organic carbon* (in Chinese). Hunan Agricultural University.
- Thilakarathna, S. K., Hernandez-Ramirez, G., Puurveen, D., Kryzanowski, L., Lohstraeter, G., Powers, L. A., Quan, N., & Tenuta, M. (2020). Nitrous oxide emissions and nitrogen use efficiency in wheat: Nitrogen fertilization timing and formulation, soil nitrogen, and weather effects. *Soil Science Society of America Journal*, 84(6), 1910–1927. <https://doi.org/10.1002/saj2.20145>
- Wang, F., Mu, Z. J., Guo, T., Huang, A. Y., Lin, X., Shi, X. J., & Ni, J. P. (2020). Effect of long-term differentiated fertilisation regimes on greenhouse gas emissions from a subtropical rice-wheat cropping system. *Plant, Soil and Environment*, 66(4), 167–174. <https://doi.org/10.17221/693/2019-Pse>
- Weller, S., Fischer, A., Willibald, G., Navé, B., & Kiese, R. (2019). N<sub>2</sub>O emissions from maize production in south-West Germany and evaluation of N<sub>2</sub>O mitigation potential under single and combined inhibitor application. *Agriculture Ecosystems & Environment*, 269, 215–223. <https://doi.org/10.1016/j.agee.2018.10.004>
- Wu, P. P. (2008). *Ammonia volatilization and nitrous oxide emission from double rice system in red paddy soil under different fertilizing systems* (in Chinese). Nanjing Agricultural University.
- Wu, S. P., Sui, F., Xiao, X. J., Zhang, J., Wu, Z. M., Zeng, Y. J., & Huang, S. (2020). Effects of different multiple cropping pattern on the global warming potential in southern double cropping rice fields (in Chinese). *Journal of Nuclear Agricultural Sciences*, 34(2), 376–382. <https://doi.org/10.11869/j.issn.100-8551.2020.02.0376>
- Xue, X. H. (2010). *Effect of fertilization on nitrate leaching and greenhouse gases emission in the typical dry-farming area* (in Chinese). Graduate University of Chinese Academy of Sciences.
- Yang, G. M. (2007). *Fluxes of CH<sub>4</sub>, CO<sub>2</sub> and N<sub>2</sub>O from paddy field in Xishuangbanna, SW China* (in Chinese). Xishuangbanna Tropical Botanical Garden of Chinese Academy of Sciences.
- Yang, Y., Tong, Y. A., Gao, P. C., Htun, Y. M., & Feng, T. (2020). Evaluation of N<sub>2</sub>O emission from rainfed wheat field in northwest agricultural land in China. *Environmental Science and Pollution Research*, 27(35), 43466–43479. <https://doi.org/10.1007/s11356-020-09133-0>
- Yu, Y. J., Gao, M. R., & Zhu, B. (2012). Comparison study on N<sub>2</sub>O emissions from field under wheat-maize rotation system and field under vegetable cultivation (in Chinese). *Acta Pedologica Sinica*, 1, 96–103.
- Zhai, L. M., Liu, H. B., Zhang, J. Z., Huang, J., & Wang, B. R. (2011). Long-term application of organic manure and mineral fertilizer on N<sub>2</sub>O and CO<sub>2</sub> emissions in a red soil from cultivated maize-wheat rotation in China. *Agricultural Sciences in China*, 10(11), 1748–1757. [https://doi.org/10.1016/S1671-2927\(11\)60174-0](https://doi.org/10.1016/S1671-2927(11)60174-0)
- Zhang, J. K., Jiang, C. S., Hao, Q. J., Tang, Q. W., Cheng, B. H., Li, H., & Chen, L. H. (2012). Effects of tillage-cropping systems on methane and nitrous oxide emissions from agro-ecosystems in a purple paddy soil (in Chinese). *Environmental Sciences*, 6, 1979–1986. <https://doi.org/10.13227/j.hjck.2012.06.041>

## SUPPORTING INFORMATION

Additional supporting information can be found online in the Supporting Information section at the end of this article.

**How to cite this article:** Shang, Z., Cui, X., van Groenigen, K. J., Kuhnert, M., Abdalla, M., Luo, J., Zhang, W., Song, Z., Jiang, Y., Smith, P., & Zhou, F. (2024). Global cropland nitrous oxide emissions in fallow period are comparable to growing-season emissions. *Global Change Biology*, 30, e17165. <https://doi.org/10.1111/gcb.17165>